

Supplementary Information

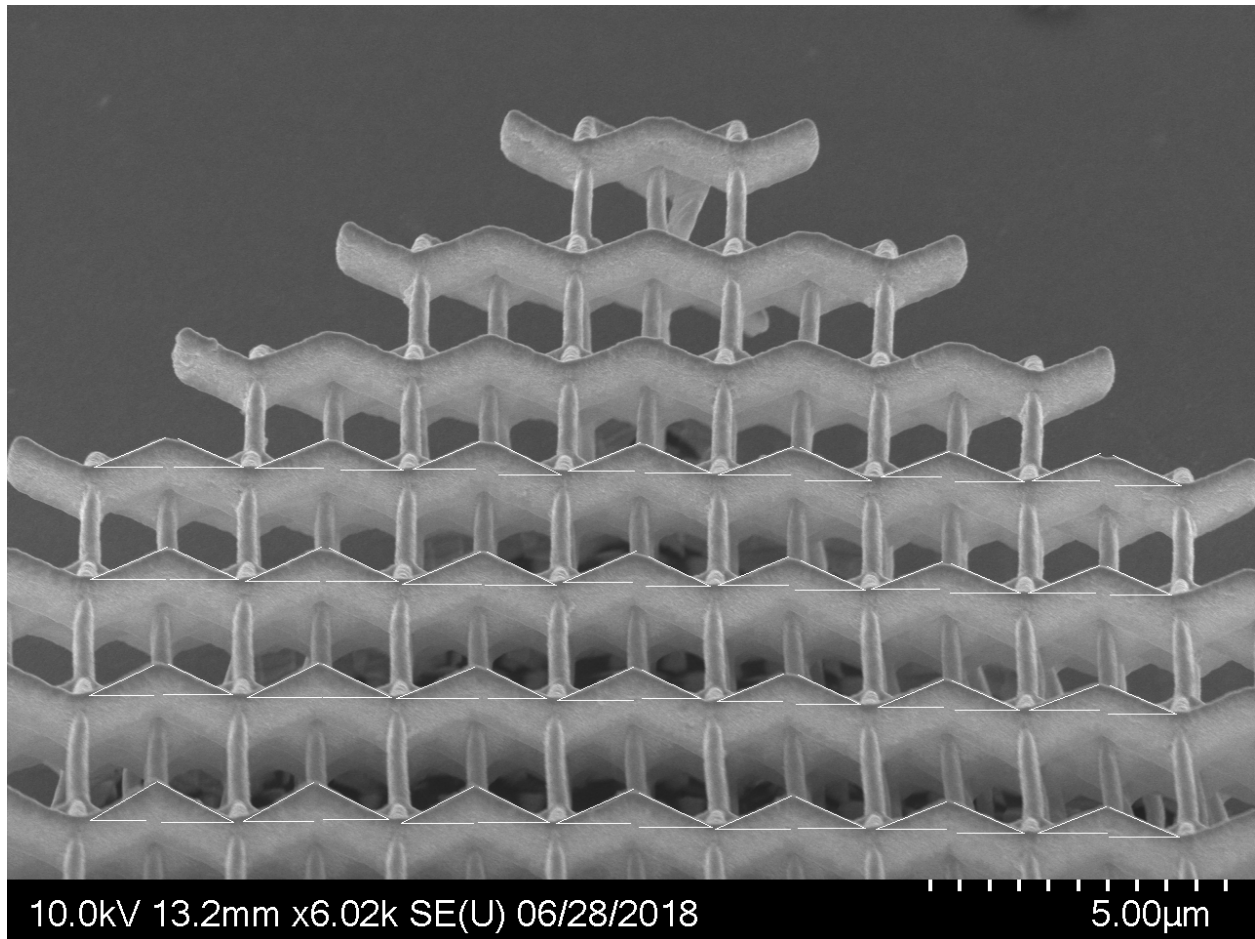
Magnetic Charge Propagation upon a 3D Artificial Spin-ice

A. May¹, M. Saccone², A. van den Berg¹, J. Askey¹, M. Hunt¹ and S. Ladak*¹

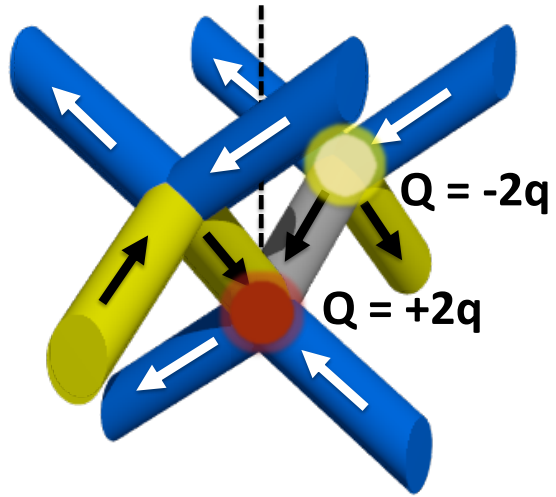
Correspondence to: ladaks@cardiff.ac.uk

This PDF file includes:

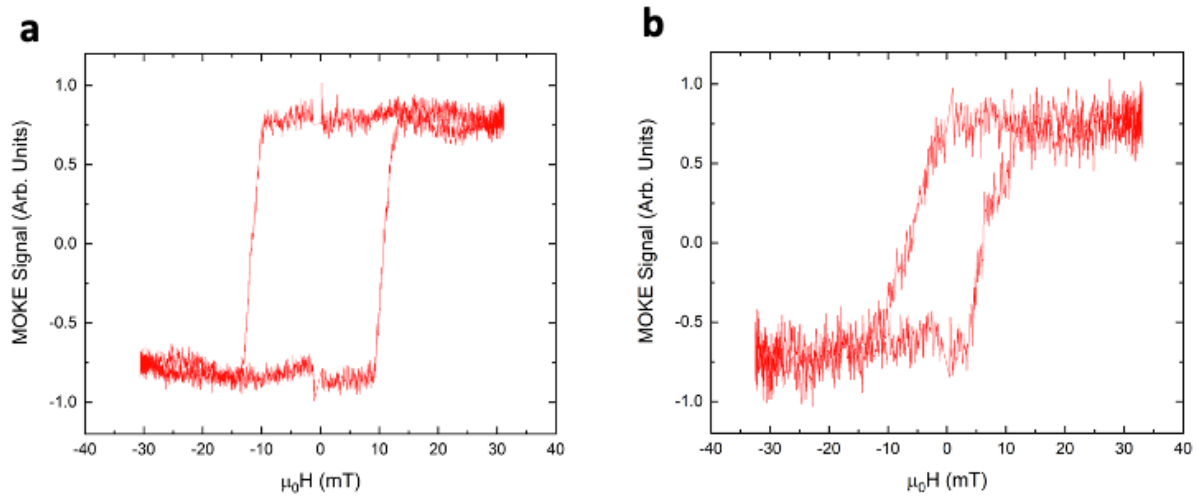
Figs. S1 to S12



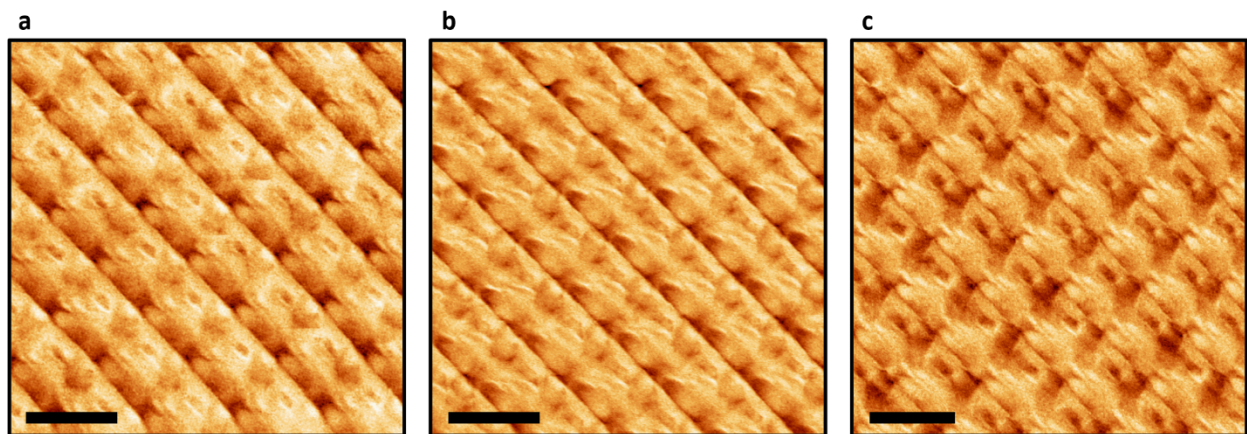
Supplementary Fig. 1: SEM image showing 50 measurements of the angle between the L1 wire long-axis and the substrate plane (θ). A simple calculation was required to transform this measured angle into the actual angle, to account for the 45° tilt present during image acquisition.



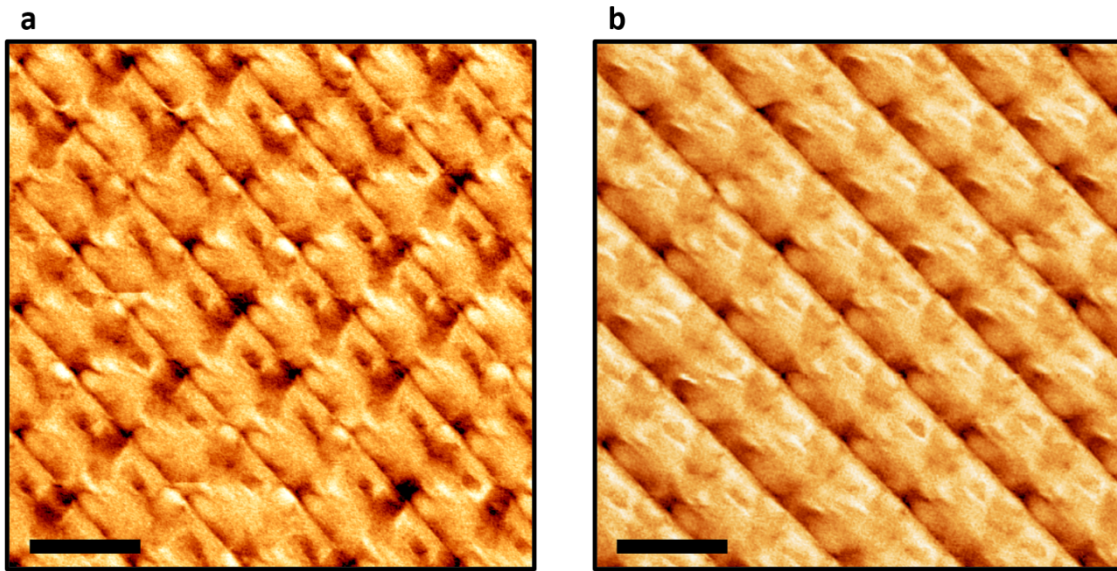
Supplementary Fig. 2: A schematic showing the creation of monopoles upon the L2 sub-lattice.



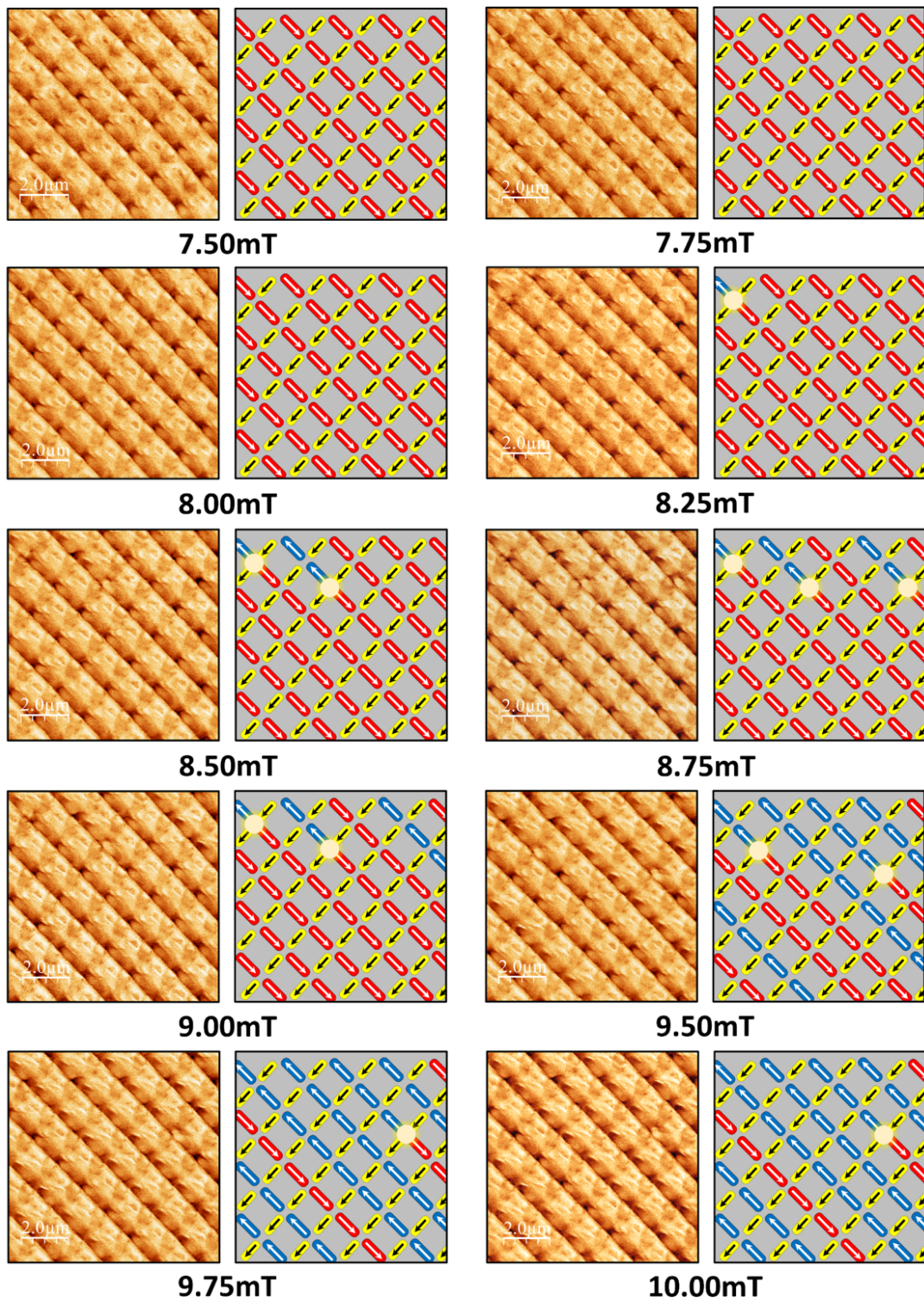
Supplementary Fig. 3: Optical magnetometry with external field applied along projection of **(a)** L1 sub-lattice and **(b)** L2 sub-lattice.



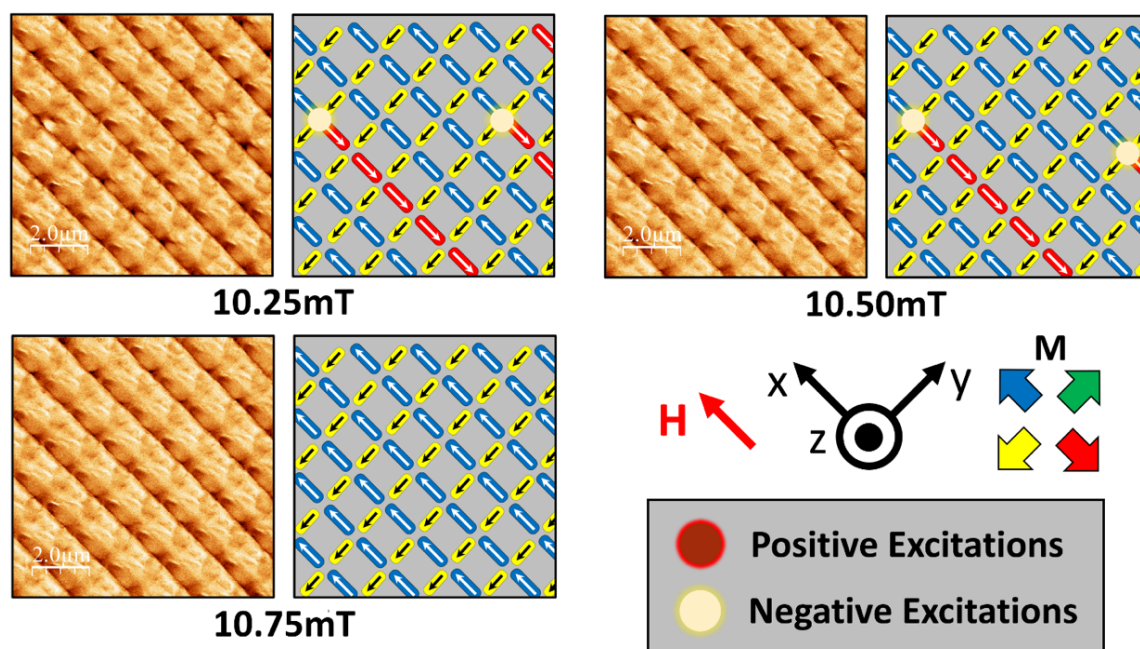
Supplementary Fig. 4: Unmasked MFM images of L1 and L2 saturated states. (a) An MFM image taken at remanence after application of saturating fields along the unit vectors $(1,-1,0)$ and $(-1,-1,0)$. (b) MFM image taken at remanence after a further saturating field is now applied along unit vector $(-1,1,0)$. (c) MFM image taken at remanence after a further saturating field is now applied along unit vectors $(1,-1,0)$ and $(1,1,0)$. See main text for definition of coordinate system. Scale bars are $2\mu\text{m}$.



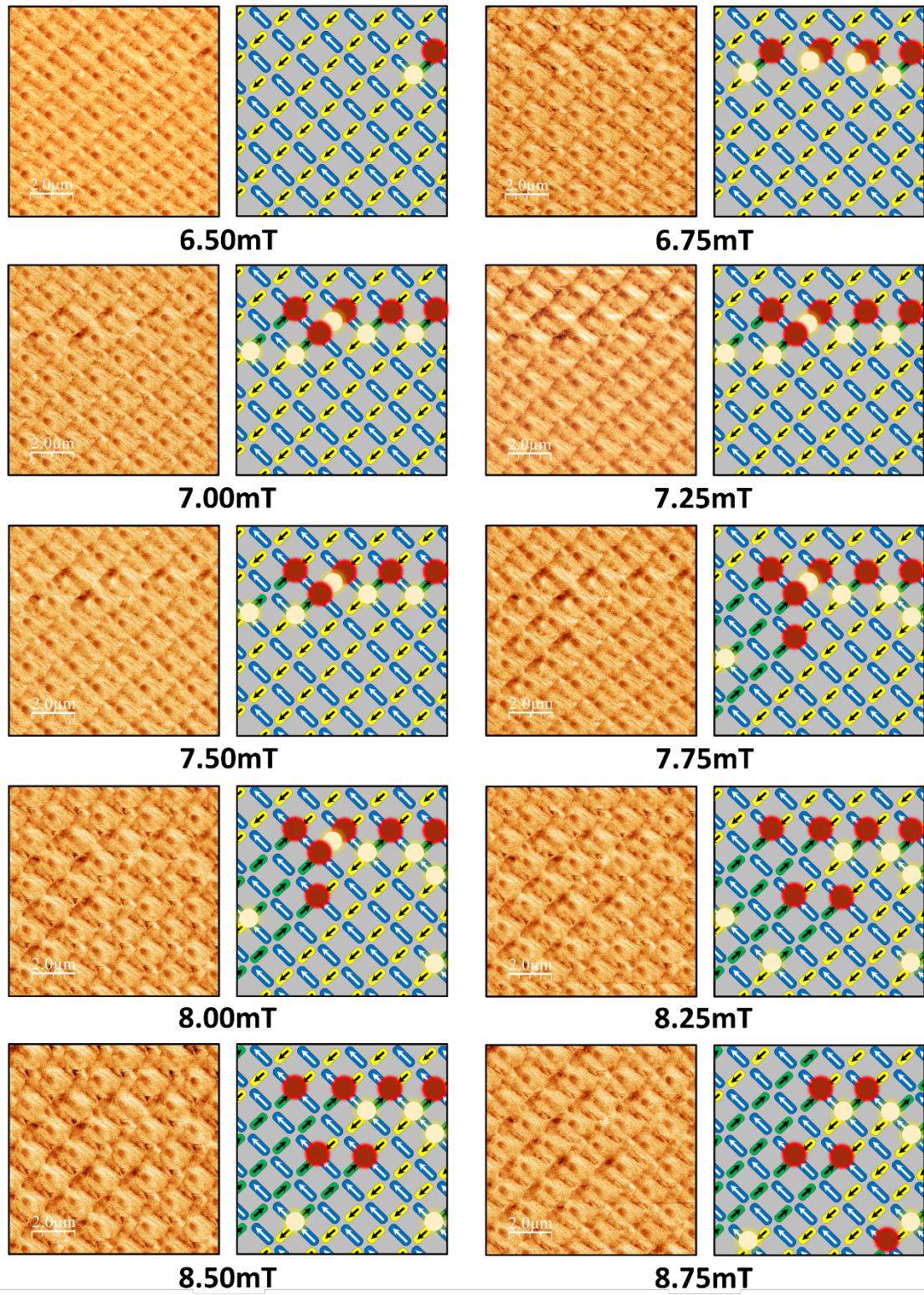
Supplementary Fig. 5: Unmasked MFM images of intermediate L1 and L2 states. (a) MFM image taken at remanence following a saturating field along L2, unit vector $(-1,-1,0)$, and subsequent 8.0mT field applied along $(1,1,0)$. (b) MFM image taken at remanence following a saturating field along L1, the unit vector $(1,-1,0)$, and subsequent 9.5mT field along the unit vector $(-1,1,0)$. See main text for definition of coordinate system.



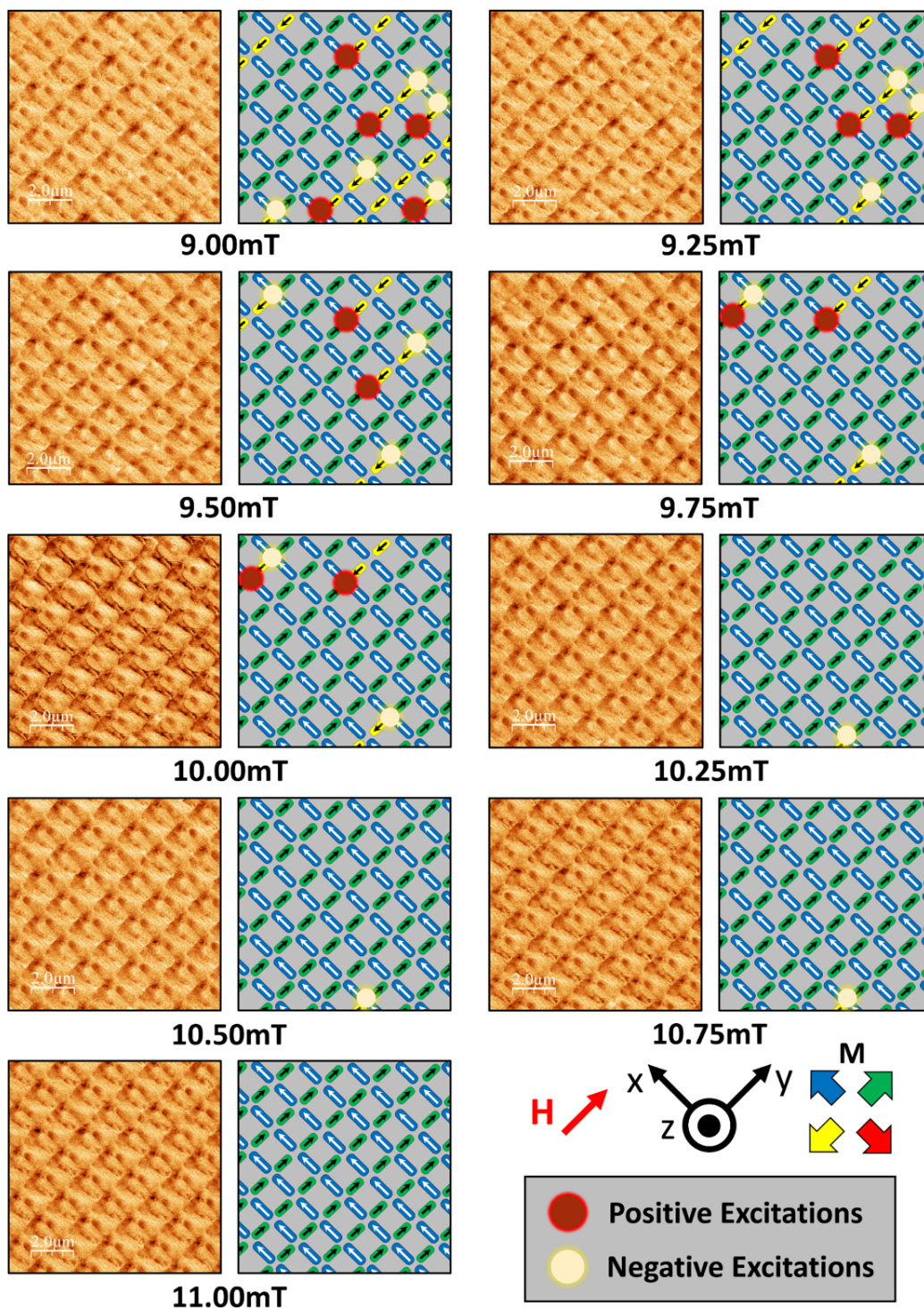
Supplementary Fig. 6: Raw MFM data without masks, L1 switching. All scale bars are 2 μ m.



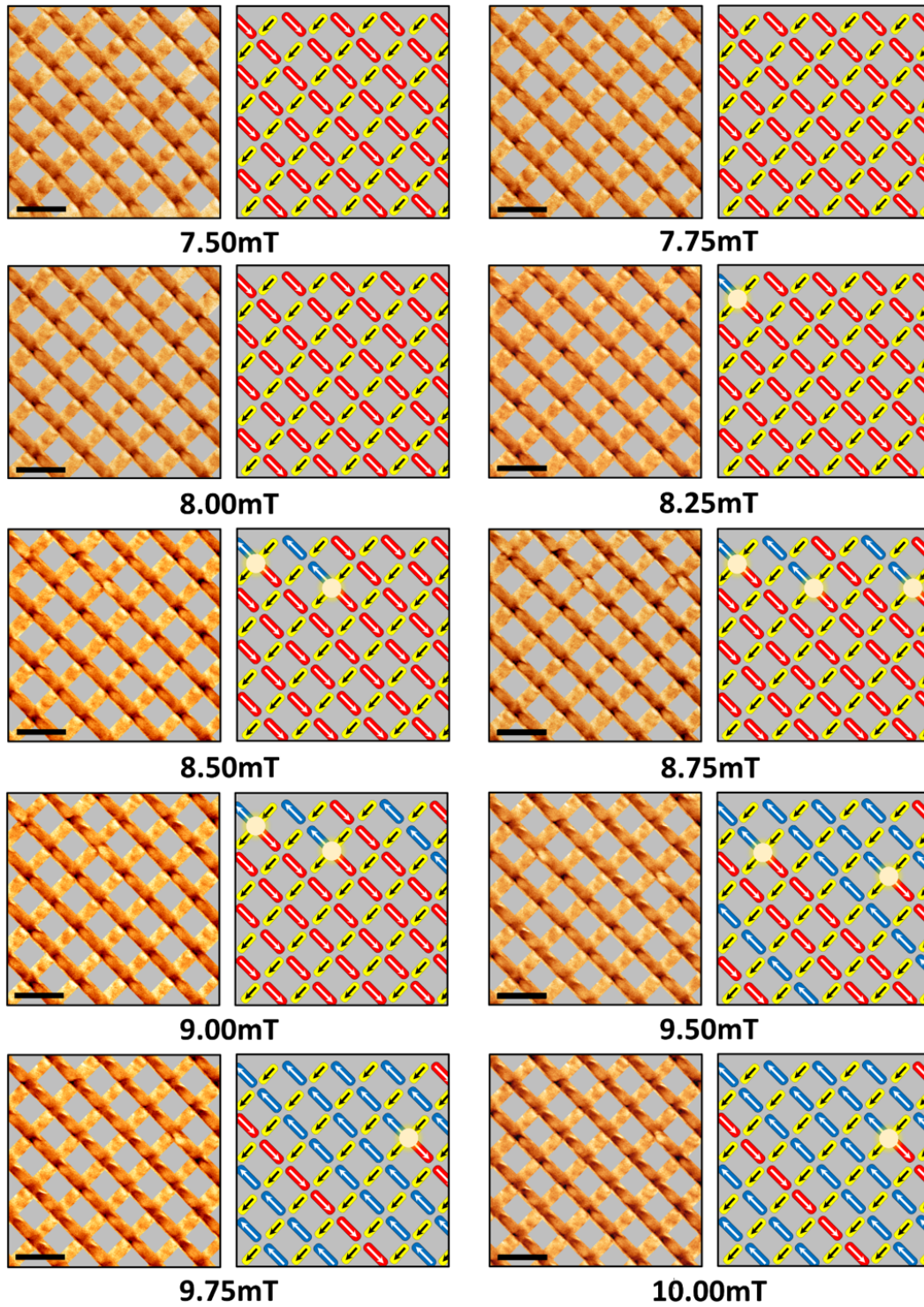
Supplementary Fig. 6 (continued): Raw MFM data without masks, L1 switching. All scale bars are 2 μm.



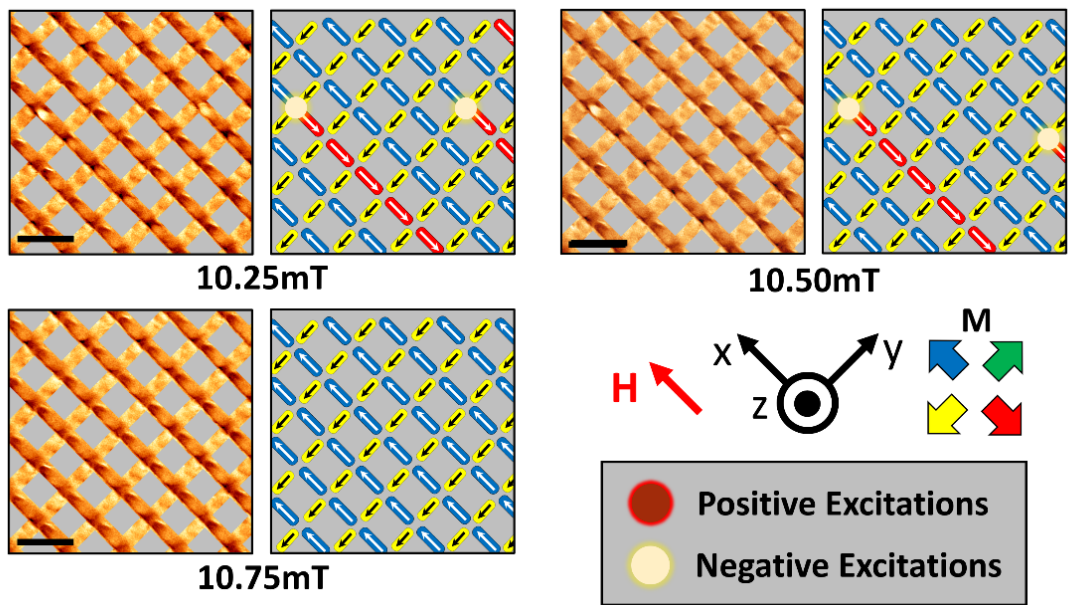
Supplementary Fig. 7: Raw MFM data without masks, L2 switching. All scale bars are 2µm.



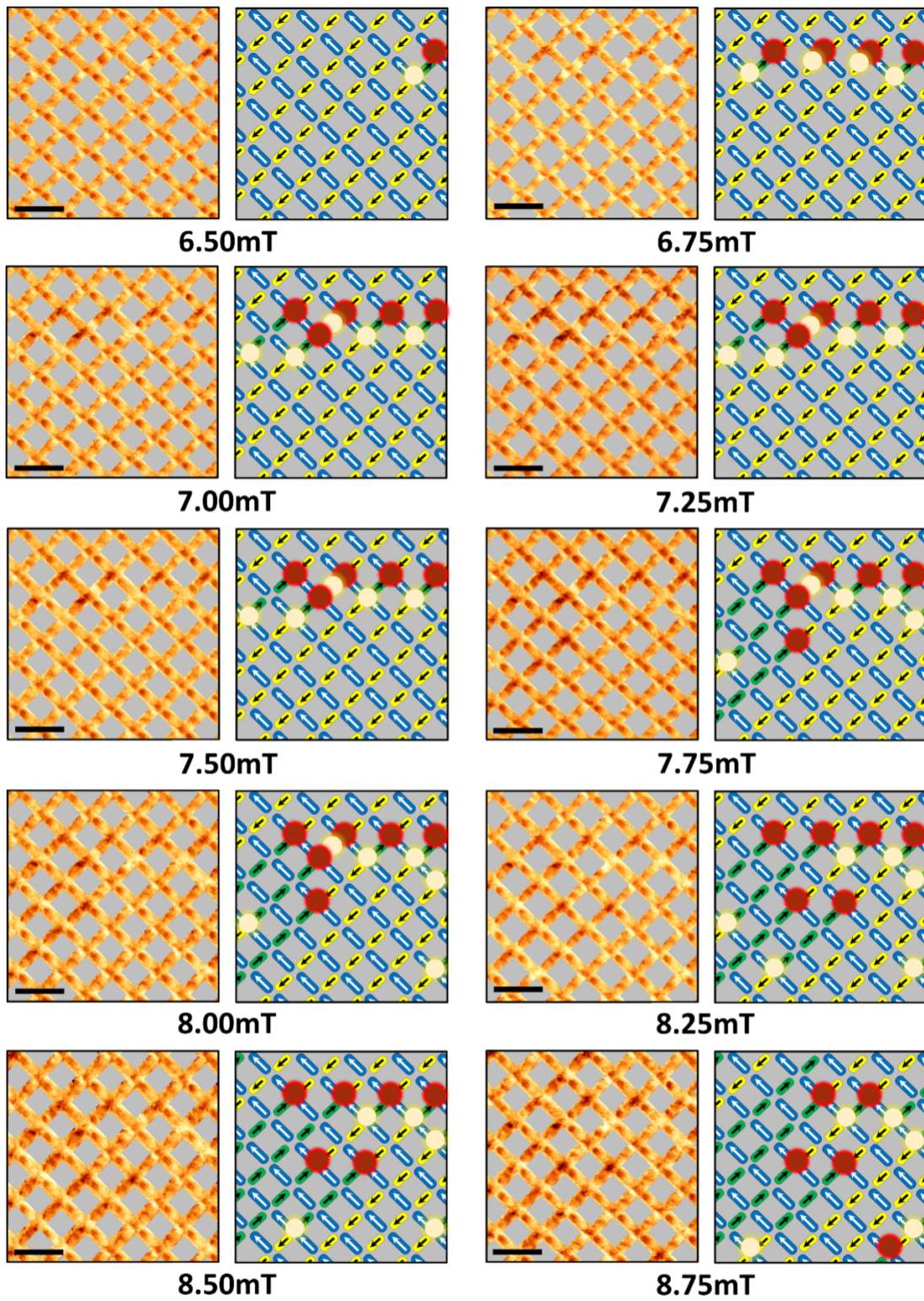
Supplementary Fig. 7 (continued): Raw MFM data without masks, L2 switching. All scale bars are 2 μ m.



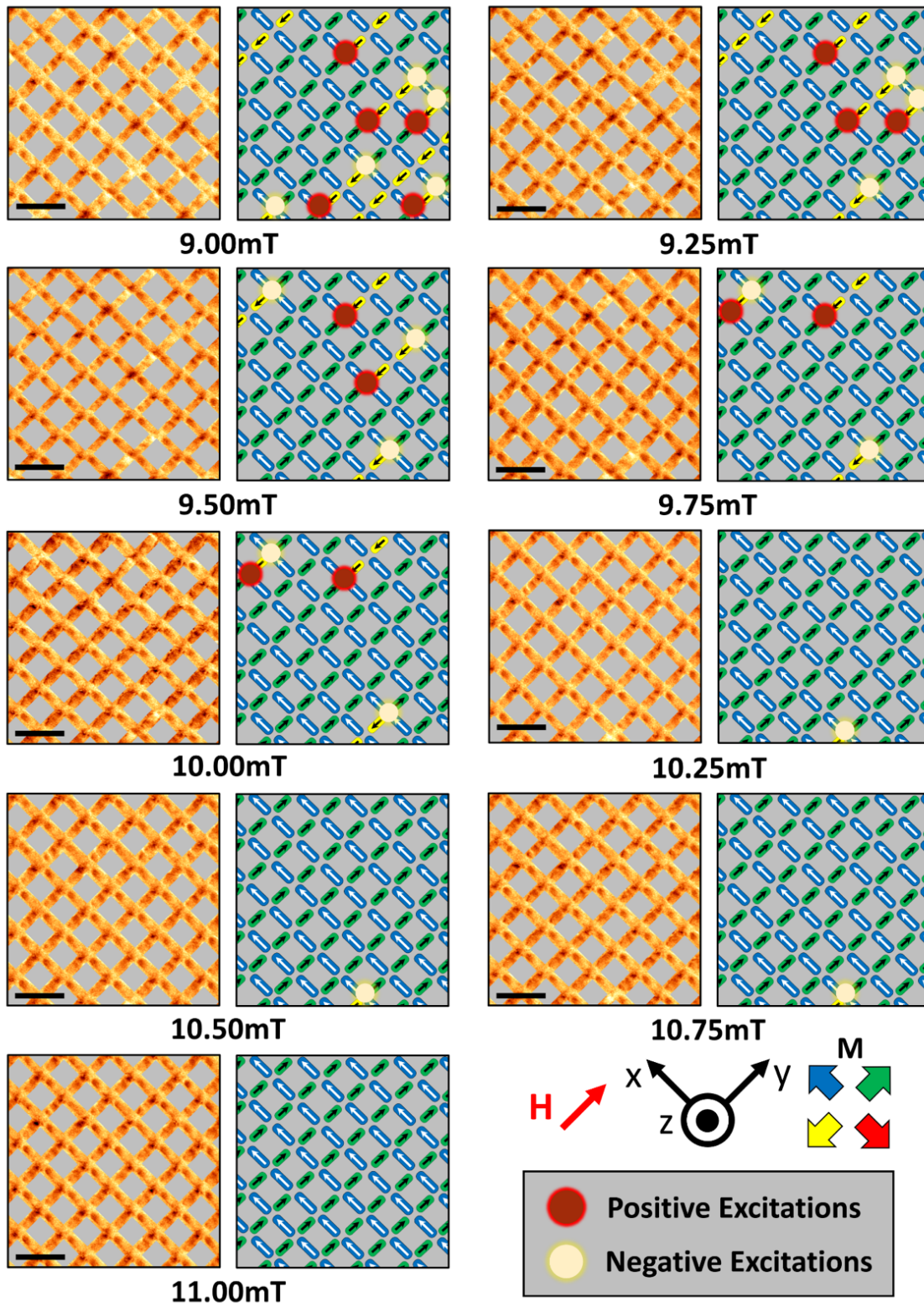
Supplementary Fig. 8: Full MFM data with masks, L1 switching. All scale bars are $2\mu\text{m}$.



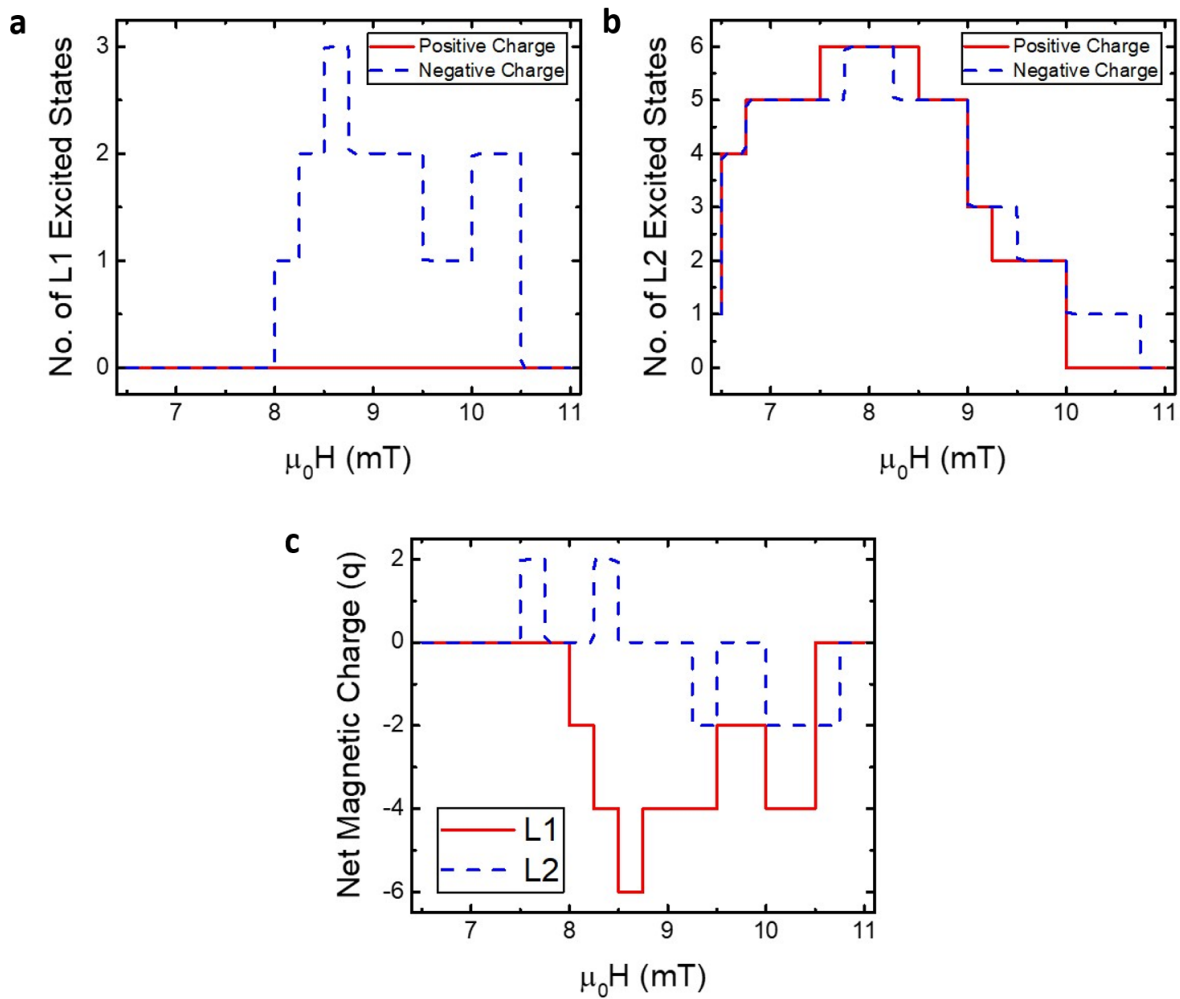
Supplementary Fig. 8 (continued): Full MFM data with masks, L1 switching. All scale bars are $2\mu\text{m}$.




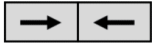
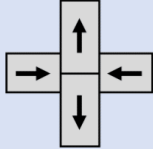
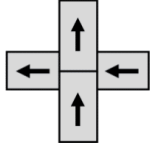
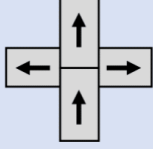
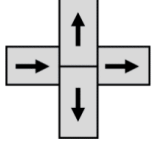
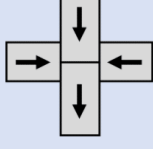
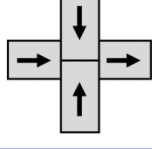
Supplementary Fig. 9: Full MFM data with masks, L2 switching. All scale bars are $2\mu\text{m}$.



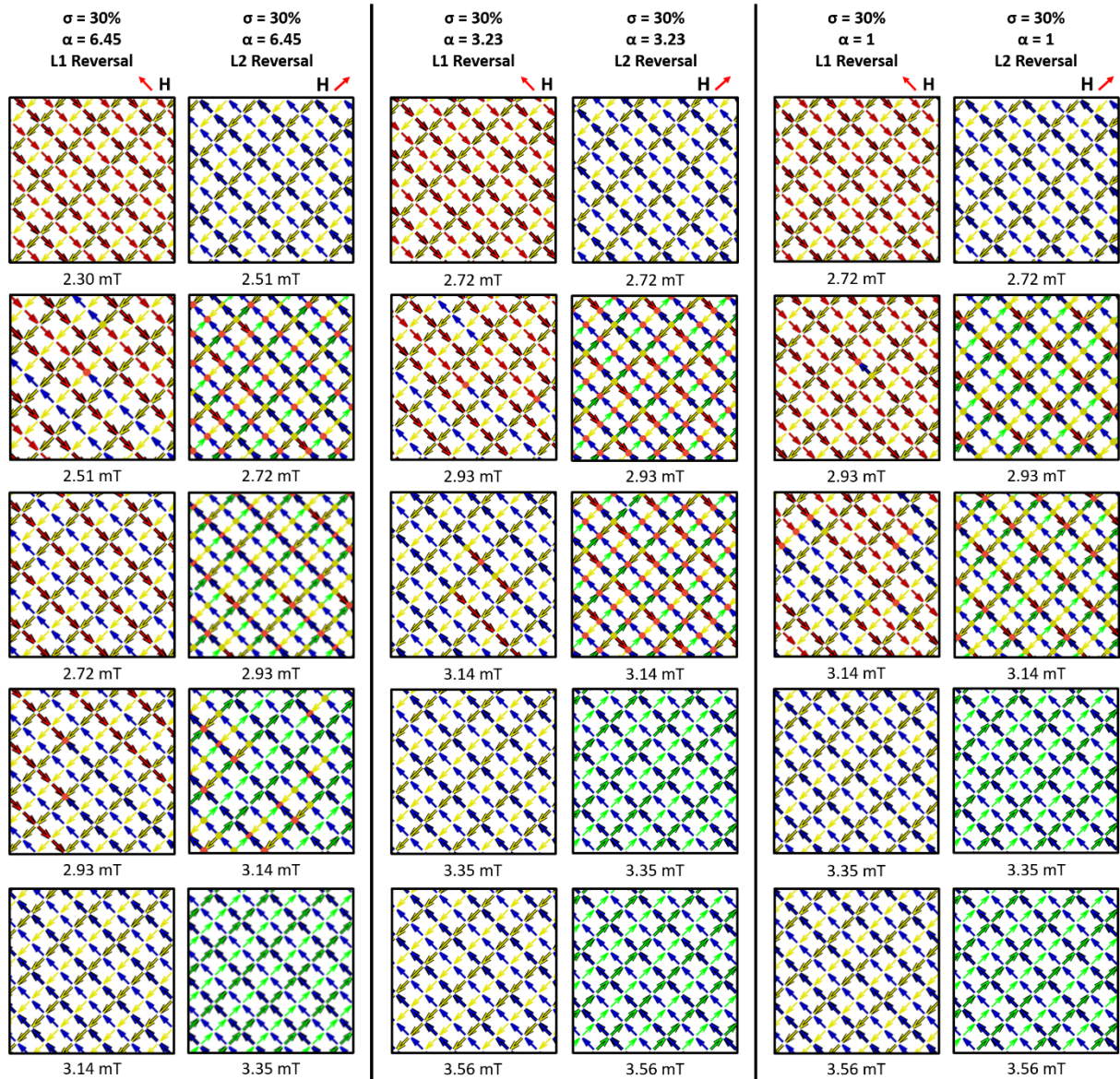
Supplementary Fig. 9 (continued): Full MFM data with masks, L2 switching. All scale bars are $2\mu\text{m}$.



Supplementary Fig. 10: Analysis of MFM reversal datasets. **(a)** Number of monopole-excitations as a function of applied field for the L1 switching. Excitations are separated into $Q = +2q$ (red) and $Q = -2q$ (blue). **(b)** Equivalent plot for observed monopole-excitations during the L2 reversal. **(c)** Net magnetic charge within the measured window during the L1 (red) and L2 (blue) reversals.

Vertex Diagram	Vertex Type	Energy Density (Jm ⁻³)
	1-in/1-out	7021
	2-in	16006
	1	8342
	2	7745
	3	9907
	3	11276
	3	10447
	3	11683

Supplementary Fig. 11: Vertex energies as calculated using micromagnetic simulations.



Supplementary Fig. 12: Full Monte-Carlo Simulations with varying surface energetics (α_{ij}). Micromagnetic simulations indicate $\alpha_{ij} = 3.23$, whereas these Monte-Carlo simulations most closely resemble the experimental results when $\alpha_{ij} = 6.45$.